Single Transverse Mode VCSELs with High Output Power Emitting in the 980 nm Wavelength Range

Ihab Kardosh and Fernando Rinaldi

We report high single-mode output powers up to 15.0 mW from vertical-cavity surface-emitting lasers (VCSELs) with curved dielectric mirrors. The VCSELs are characterized on wafer under continuous-wave operation at room temperature and show average beam quality factors $M^2 \approx 1.7$.

1. Introduction

In recent years, vertical-cavity surface-emitting lasers (VCSELs) operating in a single transverse mode have gained a growing interest in many optical fields like spectroscopy, imaging and sensing. Usually, to achieve single-mode emission in conventional oxide-confined VCSELs, the active diameter is typically scaled down to a few micrometers ($\leq 4\,\mu$m) which limits the optical output power. Furthermore, small devices suffer from ohmic heating and high current densities and thus a reduction in lifetime. Several approches including coupled resonators [1], surface etching [2], [3], and Zn-diffusion [4] have been demonstrated to control and stabilize the transverse mode emission in large ($> 4\,\mu$m) oxide-confined VCSELs. However, the maximum output power from 850 nm VCSELs is 7.5 mW with a side-mode suppression ratio of 30 dB [3]. One successful approach towards higher power is the use of an extended cavity configuration with a dielectric micromirror. Single-mode output powers of 5 mW have been achieved from monolithic 980-nm VCSELs with flat mirrors on GaAs substrates [5]. Hybrid integration of curved micromirrors on glass substrates with 980-nm VCSELs mounted on AlN heatsinks has been demonstrated with single-mode output powers of about 7 mW [6]. In this article, we present a method for the fabrication of compact vertical extended-cavity surface-emitting lasers with monolithic integration of dielectric distributed Bragg reflector (DBR) micromirrors, which is suited for wafer-scale fabrication. The single-mode bottom-emitting VCSELs have up to 15.0 mW output power in the 980 nm wavelength range.

2. Device Structure and Design

The VCSEL structures are grown by solid-source molecular beam epitaxy on a semi-insulating (SI) GaAs substrate and are designed for emission wavelengths near 980 nm. The active region contains two stacks of three 8 nm thick InGaAs/GaAs quantum wells (with half-wavelength distance) surrounded by two 30 nm thick GaAsP layers for strain compensation. The active diameter is defined by selective oxidation of a 30 nm thick AlAs

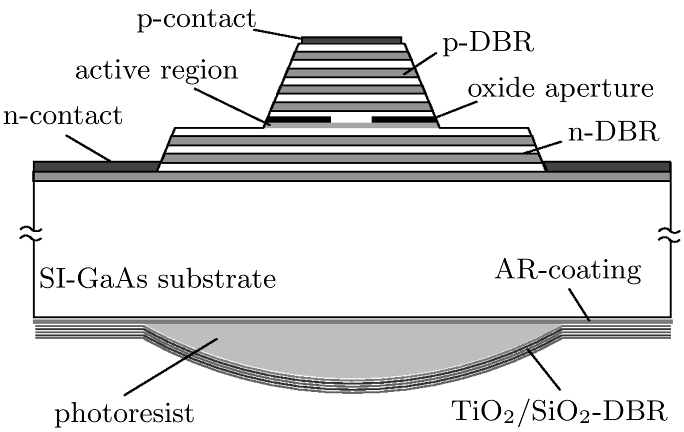

Fig. 1: Schematic cross-section of the monolithically integrated VCSEL.

layer above the active region, located in a node of the standing-wave pattern. The VCSEL contains a 30 pairs p-doped DBR and a 3 pairs n-doped DBR for wavelength selection. A schematic cross-section of the device is shown in Fig. 1. The spherical shape of the photoresist surface is designed to fit the radius of curvature R of the output beam which is calculated as

$$R = \frac{n_2}{n_1} L \left[1 + \left(\frac{Z_\mathrm{R}}{L} \right)^2 \right] \text{ with } Z_\mathrm{R} = \frac{\pi W_0^2 n_1}{M^2 \lambda} \tag{1}$$

additionally considering the refractive indexes $n_1 = 3.52$ and $n_2 = 1.53$ of GaAs and photoresist, respectively. Z_R is the Rayleigh length, L the substrate thickness, W_0 the radius of the beam waist, λ the vacuum wavelength and M^2 the beam quality factor. To avoid beam clipping, the diameter of the micromirror should be larger than the output beam diameter. In case of an extended cavity length of 150 µm, the Rayleigh length of the fabricated devices approximately ranges from L to $3L$ depending on W_0, hence the beam diameter at the output mirror is not much larger than in the active region. The dielectric DBR consists of 9 layers of TiO_2 and SiO_2 which are deposited on the photoresist using an ion-beam sputter deposition system. The mirror is designed to provide a high reflectivity of 97 % near 970 nm wavelength.

3. Device Fabrication

The fabricated VCSELs are bottom emitters with circular p-type contacts on the top of the mesa and have active diameters from 9 to 16 µm. The semi-insulating substrate that is used to minimize the free-carrier optical loss demands the fabrication of intracavity n-contacts on the epitaxial side. Large-area n-metallization layers are evaporated on the partly etched n-DBR as illustrated in Fig. 1. The substrate is thinned to approximately 150 µm before depositing a TiO_2 anti-reflection (AR) coating. The curved micromirrors are fabricated by using a technology known from microlenses. Polyimide and PMGI photoresists have been used for microlens formation on GaAs substrates of 980 nm VCSELs for decreasing the beam divergence [7, 8]. We have chosen PMGI photoresist due to its optical transparency in the near infrared and its excellent reflow properties. The PMGI is patterned into round disks using a two-step lithographical process, followed by thermal reflow at 290 °C that transforms the disks into spherical lenses. The radius of curvature of the lens depends on the diameter and the thickness of the initial disk. Microlens diameters from 100 to 150 µm are used, resulting in radii of curvature of about 0.8 to 2 mm.

4. Experimental Results and Discussions

The output characteristics of monolithically integrated VCSELs with different active diameters D_a are shown in Fig. 2.

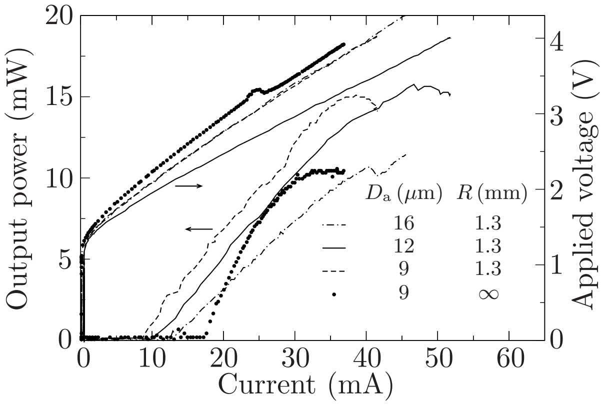

Fig. 2: Output characteristics of VCSELs with different active diameters D_a and radii of curvature R, measured on wafer at room temperature.

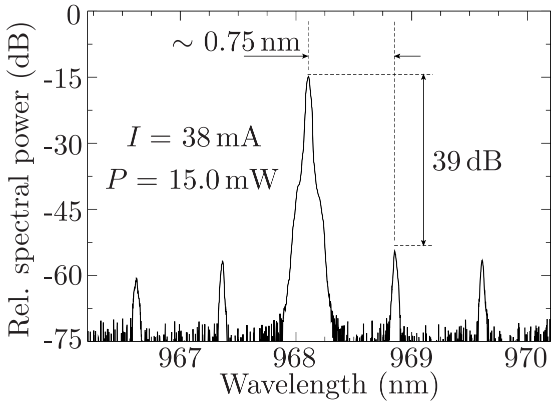

Fig. 3: Emission spectrum of the 9 µm diameter VCSEL ($R = 1.3$ mm) in Fig. 2 measured at 38 mA (15.0 mW).

The 9 µm diameter device ($R = 1.3$ mm) has a threshold current I_th of 7.5 mA and shows stable single transverse and longitudinal mode operation from threshold to rollover with a maximum single-mode output power $P_\mathrm{max,SM}$ of 15.0 mW and a side-mode suppression ratio of 39 dB, as evidenced by the optical spectrum in Fig. 3. The separation of 0.75 nm between the modes corresponds to the longitudinal mode spacing of a 150 µm long Fabry–Pérot resonator. All spectra were taken with a resolution of 0.01 nm. The ripples in the output curves, especially for small devices, can be attributed to laser heating, namely a varying temperature alters both the emission wavelength and the optical path length between the partial n-DBR and the dielectric mirror. In general, on-wafer measurements of bottom emitters induce strong device heating, owing to the lack of a direct contact with a heatsink. Almost all VCSELs with larger active diameter also exhibit single-mode operation, however, with higher threshold current and reduced differential quantum effeciency η_d, resulting in a lower output power compared to the 9 µm diameter device with the same radius of curvature. Independent of the device size, the VCSELs can show longitudinal multimode oscillation. In Fig. 2, this occurs mainly close to rollover. The small drop observed in the output power curve of the 16 µm diameter VCSEL is due to such a second mode which appears around 41 mA, as can be seen in Fig. 4 (right). In addition to the curved output mirrors, flat mirrors have also been fabricated.

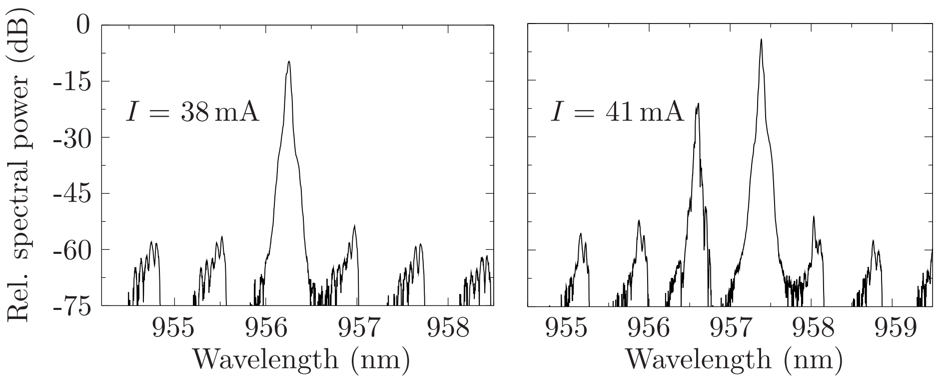

Fig. 4: Emission spectra of the 16 µm diameter device in Fig. 2 measured at 38 mA (left) and 41 mA (right). The transverse mode behavior of the longitudinal side modes is clearly observed.

The output characteristics of a 9 µm diameter device with a flat mirror ($R \to \infty$) are included in Fig. 2. The VCSEL shows single-mode emission but has a higher threshold current compared to the corresponding device with curved mirror. Increasing the radius of curvature decreases the optical feedback into the active region, which leads to higher threshold currents. Simultaneously, higher differential quantum efficiencies are observed. This behavior can be attributed to thermal lensing, which reduces the diffraction losses with increasing current. Experimental parameters of the VCSELs in Fig. 2 are listed in Table 1. In Fig. 5, calculated beam quality factors M^2 according to (1) are plotted against the radius of curvature of the output mirror. The symbols indicate averaged M^2 values obtained from beam quality measurements performed on several comparable single-mode devices. The observed range of M^2 can be attributed to beam waist diameters between 17 and 22 µm, as shown in Fig. 5, where thermal lensing is not considered. The beam profile of the 16 µm diameter device with $M^2 = 1.58$ is shown in Fig. 6. In general, VCSELs with small active diameters around 9 µm show stable single-mode operation with radii of curvature $\geq$ 0.8 mm. For active diameters of 16 µm or larger, radii of curvature $\geq$ 1.3 mm are required to obtain comparable beam quality factors and stable single-mode emission. The extended cavity length limits the maximum active diameter that allows single-mode emission. With increasing length of the extended cavity, a reduction of beam quality factors is expected from (1) for $L < n_1R/(2n_2)$. For a 300 µm thick substrate, we have obtained average $M^2 = 1.5$ instead of 1.7 (with $L = 150$ µm) for comparable devices.

Table 1: Experimental parameters of VCSELs in Fig. 2.

D_a (µm)	I_th (mA)	$P_\mathrm{max,SM}$ (mW)	η_d (%)	R (mm)
9	7.5	15.0	41	1.3
9	16.0	10.0	66	∞
12	10.2	13.9	40	1.3
16	12.3	10.0	32	1.3

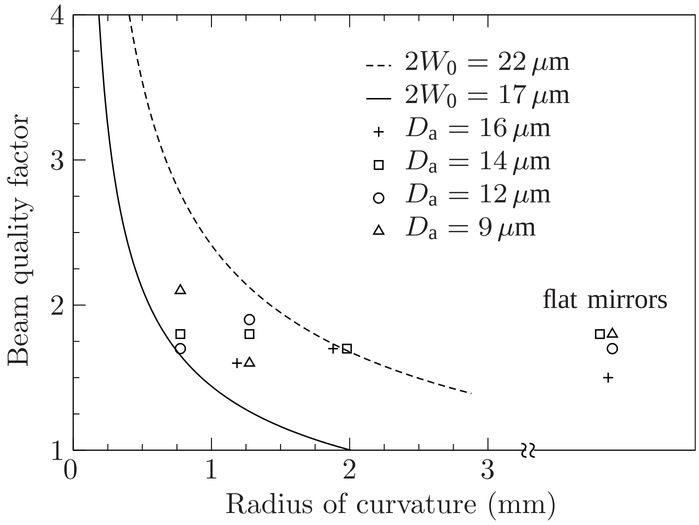

Fig. 5: Calculated beam quality factors versus the radius of curvature of the mirror for different beam waist diameters $2W_0$, where a substrate thickness of 150 µm and a wavelength of 965 nm are assumed. Measurement results obtained from various single-mode devices are shown as symbols.

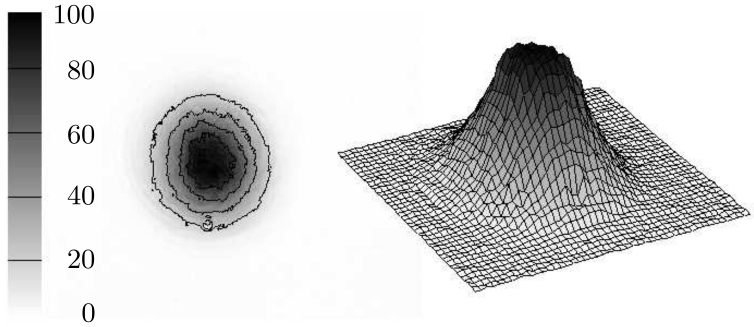

Fig. 6: Contour plot and three-dimensional plot of the beam profile of the 16 µm diameter VCSEL measured at 38 mA (10.0 mW) with $M^2 = 1.58$.

5. Conclusion

Monolithic integration of micromirrors with InGaAs VCSELs is demonstrated. The compact lasers operate at room temperature in a stable single mode with continuous wave output powers up to $P = 15.0$ mW. The combination of the epitaxial VCSEL cavity with the extended cavity allows the filtering of a single longitudinal mode together with fundamental transverse mode operation. Beam quality measurements yield an average M^2 of 1.7 and a radiance $P/(\lambda M^2)^2$ of more than 5×10^5 W/(cm^{2}sr). The structure and design presented here demonstrates the feasibility to realize single-mode VCSELs with maximum output powers exceeding those reported so far. Furthermore, the small device dimension is compatible with standard packaging. In an alternative approach which simplifies the device structure, the shape of the photoresist can be transformed into the substrate by applying an adequate dry-etching technique. Finally, we expect a higher performance with a more appropriate mounting technique that ensures efficient cooling.

References

[1] A.J. Fischer, K.D. Choquette, W.W. Chow, A.A. Allerman, D.K. Serkland, and K.M. Geib, "High single-mode power observed from a coupled-resonator vertical-cavity laser diode," *Appl. Phys. Lett.*, vol. 79, no. 25, pp. 4079–4081, Dec. 2001.

[2] A. Kroner, F. Rinaldi, J.M. Ostermann, and R. Michalzik, "High-performance single fundamental mode AlGaAs VCSELs with mode-selective mirror reflectivities," *Opt. Commun.*, vol. 270, no. 2, pp. 332–335, Feb. 2007.

[3] A. Furukawa, S. Sasaki, M. Hoshi, A. Matsuzono, K. Moritoh, and T. Baba, "High-power single-mode vertical-cavity surface-emitting lasers with triangular holey structure," *Appl. Phys. Lett.*, vol. 85, no. 22, pp. 5161–5163, Nov. 2004.

[4] J.-W. Shi, C.-C. Chen, Y.-S. Wu, S.-H. Guol, C. Kuo, and Y.-J. Yang, "High-power and high-speed Zn-diffusion single fundamental-mode vertical-cavity surface-emitting lasers at 850-nm wavelength," *IEEE Photon. Technol. Lett.*, vol. 20, no. 13, pp. 1121–1123, Jul. 2008.

[5] E.M. Strzelecka, J.G. McInerney, A. Mooradian, A. Lewis, A.V. Shchegrov, D. Lee, J.P. Watson, K.W. Kennedy, G.P. Carey, H. Zhou, W. Ha, B.D. Cantos, W.R. Hitchens, D.L. Heald, V.V. Doan, and K.L. Lear, "High power, high brightness 980 nm lasers based on the extended cavity surface emitting lasers concept," *Proc. SPIE*, vol. 4993, pp. 57–67, Jan. 2003.

[6] M.W. Wiemer, R.I. Aldaz, D.A.B. Miller, and J.S. Harris, "A single transverse-mode monolithically integrated long vertical-cavity surface-emitting laser," *IEEE Photon. Technol. Lett.*, vol. 17, no. 7, pp. 1366–1368, Jul. 2005.

[7] O. Blum, S.P. Kilcoyne, M.E. Warren, T.C. Du, K.L. Lear, R.P. Schneider, Jr., R.F. Carson, G. Robinson, and F.H. Peters, "Vertical-cavity surface-emitting lasers with integrated refractive microlenses," *Electron. Lett.*, vol. 31, no. 1, pp. 44–45, Jan. 1995.

[8] E.M. Strzelecka, G.D. Robinson, M.G. Peters, F.H. Peters, and L.A. Coldren, "Monolithic integration of vertical-cavity laser diodes with refractive GaAs microlenses," *Electron. Lett.*, vol. 31, no. 9, pp. 724–725, Apr. 1995.